Electromechanical Coupling Model of Gating the Large Mechanosensitive Ion Channel (MscL) of *Escherichia coli* by Mechanical Force

Liqun Gu, Weihong Liu, and Boris Martinac
Department of Pharmacology, University of Western Australia, Nedlands WA 6907, Australia

ABSTRACT We have developed a theoretical electromechanical coupling (EMC) model of gating of the large-conductance mechanosensitive ion channel (MscL). The model presents the first attempt to explain the pressure-dependent transitions between the closed and open channel conformations on a molecular level by assuming 1) a homohexameric structural model of the channel, 2) electrostatic interactions between various domains of the homohexamer, 3) structural flexibility of the N-terminal portion of the monomer, and 4) mechanically and electrostatically induced displacement of the N-terminal domain relative to other structural domains of the protein. In the EMC model, 12 membrane-spanning α-helices (six each of the M1 and M2 transmembrane domains of the MscL monomer), are envisaged to line the channel pore with a diameter of 40 Å, whereas the N- and C-termini are oriented toward each other inside the pore when the channel is closed. The model proposes that stretching the membrane bilayer by mechanical force causes the monomers to be pulled away from and slightly tilted toward each other. This relative movement of α-helices could serve as a trigger to initiate a "swing-like" motion of the N-terminus around the glycine residue G14 that may act as a pivot. The analysis of the attractive and repulsive coulomb forces between all domains of the channel homohexamer suggested that an inclination angle of $\sim$3.0°–4.1° between the oppositely oriented channel monomers should suffice for the N-terminus to turn away from other domains causing the channel to open. According to the EMC model the minimal free energy change, ΔG, that could initiate the opening of the channel was 2 kT. Also, the model predicted that the negative pressure required for channel open probability, $P_o = 0.5$, should be between 50 and 80 mmHg. These values were in a good agreement with the experimentally estimated pressures of 60–70 mmHg obtained with the MscL reconstituted in liposomes. Furthermore, consistent with a notion that the N-terminus may present a mechanosensitive structural element providing a mechanism to open the MscL by mechanical force, the model provides a simple explanation for the variations in pressure sensitivity observed with several MscL mutants having either deletions or substitutions in N- or C-terminus, or site-directed mutations in the S2-S3 loop.

INTRODUCTION

Mechanosensation is an essential and diverse type of sensory transduction that is widely spread in living cells belonging to organisms of various phylogenetic origin. Mechanosensitive (MS) ion channels have been thought to be the primary molecular biosensors that may function as mechanoelectrical switches at the basis of mechanosensation in such diverse physiological processes as touch, hearing, proprioception, or embryogenesis, as well as turgor control in plant cells and osmoregulation in bacteria (Sachs, 1992; Martinac, 1993; Sackin, 1995; García-Anoverños and Corey, 1997). The ubiquity of MS channels further supports the notion of an important physiological role for this type of channels in these cellular processes (Sachs, 1988, 1992; Morris, 1990; Martinac et al., 1992; Martinac, 1993; Sackin, 1995; Hamill and McBride, 1996).

The MS channels have been extensively studied in both Gram-negative and Gram-positive bacteria (Martinac et al., 1992). Three types of MS channels have been documented in *Escherichia coli*: 1) Mechanosensitive channel of Large conductance (MscL), 2) Mechanosensitive channel of Small conductance (MscS), and 3) Mechanosensitive channel of Mini conductance (MscM) (Martinac et al., 1987, 1992; Sukharev et al., 1993, 1994a, 1997; Berrier et al., 1996). In particular, since it is the only MS ion channel with the known primary amino acid sequence and the corresponding gene, *mscL* (Sukharev et al., 1994a,b; Hamill and McBride, 1994) encoding the channel protein whose mechanosensitivity has been unambiguously documented (García-Anoverños and Corey, 1997), the MscL has been well characterized at the molecular level.

To understand the MscL mechanosensitivity, structure and function relationship of the wild-type and various recombinant MscL mutants have been studied by the patch clamp technique (Hamill et al., 1981) using both in situ (Blount et al., 1996a,b) and in vitro preparations (Häse et al., 1995, 1997). Deletion or substitution of the first eight amino acids in the N-terminus (Häse et al., 1997) or deletion of 12 initial N-terminal residues (Blount et al., 1996a) resulted in channels exhibiting altered gating and pressure sensitivity. Site-directed N-terminal mutations in the G14 residue also resulted in channels with altered gating and pressure sensitivity. Moreover, a deletion of the G14 residue caused a complete loss of mechanosensitivity of MscL, since the activity of these mutant channels was independent of the applied pressure (Liu, Gu, Deitmer and Martinac, in preparation). These results indicated the importance of the

Received for publication 9 December 1997 and in final form 10 March 1998.

Address reprint requests to Dr. Boris Martinac, Department of Pharmacology, University of Western Australia, Nedlands WA 6907, Australia. Tel.: (618) 9346-2968; Fax: (618) 9346-3469; E-mail: bmartinac@receptor.pharm.uwa.edu.au.

0006-3495/98/06/2889/14 $2.00

N-terminus, and of the G14 residue in particular, for gating and pressure sensitivity of MscL. A deletion of 27 amino acids for the C-terminus did not affect the function of the MscL channels, whereas a deletion of 33 C-terminal amino acids that included a charged cluster of five amino acids (RKKEE) abolished the channel activity (Blount et al., 1996b; Häse et al., 1997). This result indicated a particular importance of this group of charged amino acids for channel activity. Also, site-directed mutagenesis of other charged and polar residues present in the MscL amino acid sequence, such as the lysine K31 of the first transmembrane helix M1 or the glutamine Q56 of the periplasmic S2-S3 loop, revealed the overall importance of charged residues for the mechanosensitivity of the MscL (Blount et al., 1996b,c).

How the MscL is operated by the mechanical force transmitted exclusively via membrane lipid bilayer remains poorly understood. In the present study, we propose the electromechanical coupling (EMC) model of MscL gating. By emphasizing the significance of the N- and C-termini for channel gating as well as the importance of the attractive and repulsive coulomb forces between the various MscL structural domains, the model suffices to explain most of the pressure-sensitive behavior of the wild-type and several mutants of the MscL that have been investigated to date.

METHODS

Model prerequisites

The EMC model is based on several assumptions, proposed MscL tertiary structure, and presently available experimental evidence that all can be summarized as follows:

1. The MscL protein alone is necessary and sufficient for the activity of the large conductance MS ion channel of *E. coli* (Sukharev et al., 1994a);
2. The membrane tension γ that gates the MscL can be calculated for an ideal biological membrane described by lipid bilayer alone, since the MscL remains fully functional upon reconstitution into liposomes (Häse et al., 1995);
3. The proposed membrane spanning model of the MscL monomer consists of five domains that include the S1 amphipathic N-terminal domain, two membrane-spanning α-helical domains M1 and M2, another amphipathic S2-S3 domain, and a hydrophilic C-terminal domain (Fig. 1) (Blount et al., 1996a; Sukharev et al., 1996, 1997); consequently the MscL belongs to a new family of structurally related ion channels having two membrane spanning α-helices (North, 1996);
4. The functional MscL channel is a homohexamer (Blount et al., 1996a; Sukharev et al., 1996, 1997) with a pore size of ~40 Å (Cruickshank et al., 1997);
5. All 12 α-helices of the MscL homohexamer line the pore of the channel (Cruickshank et al., 1997);
6. Deletions and amino acid substitutions in the N-terminal domain strongly affect the channel pressure sensitivity and gating properties (Blount et al., 1996a; Häse et al., 1997);
7. Deletions in the C-terminal domain region affect gating properties of the channel to a lesser extent, except when a deletion included a charged group of five amino acids (RKKEE) that resulted in complete abolishment of channel activity (Blount et al., 1996a; Häse et al., 1997);
8. Site-directed mutations that affect the overall net electric charge of any of the channel domains (Blount et al., 1996b), may cause changes in the pressure sensitivity as well as channel gating kinetics of the MscL;
9. Structural flexibility of the N-terminal domain may be provided by the glycine G14 located at the interface between the N-terminus and M1 α-helix, since glycine residues may exhibit many different conformations in various unfolded protein structures (Branden and Tooze, 1991), such as the putative link between the N-terminus and the M1 helix (Fig. 1);
10. Attractive and repulsive electrostatic coulomb forces exist between various domains of the channel.

In the proposed EMC gating model the strategically positioned equivalent net charges within each single domain of MscL are considered to be the source of coulomb forces responsible for conformational changes underlying closed-open transitions of the channel when the membrane is stretched. From the helical wheel representation of M1 and M2 α-helices (Fig. 1 *B*), one side of the α-helix (right side of the M1 domain and left of the M2 domain relative to the dashed line in Fig. 1 *B*) is more charged and therefore possibly overall more hydrophilic than the other side of the helix. The hydrophilic side may be envisioned as facing the aqueous phase inside the pore of the functional MscL channel that was proposed to be a homohexamer (Sukharev et al., 1996, 1997). Similarly, the N-terminus has amphipathic properties by being hydrophilic on one side and less hydrophilic on the other, as shown in its helical wheel representation (Fig. 1 *B*). According to the EMC model proposed in this study, the hydrophilic side of N-terminus faces the aqueous extramembranous environment and the less hydrophilic side is oriented toward the pore (Fig. 2 *B*). Although the water in the large MscL pore may be expected to be equivalent to bulk water, this orientation of the N-terminus is reasonable to assume, since in this orientation arginine R8 provides the N-terminus with a net positive charge. Consequently, the less hydrophilic side can be kept in a position parallel to the membrane bilayer by attractive electrostatic forces inside the channel pore, thus keeping the channel closed.

Another assumption required by the EMC model is the rotational flexibility of the N-terminus. According to the membrane spanning model of the MscL (Fig. 1) the N-terminus is linked to the M1 domain through the glycine residue G14. Generally, glycine residues provide proteins with flexibility, since they may exhibit many different conformations in various unfolded protein structures (Branden and Tooze, 1991). Such may be the putative link between the N-terminus and the M1 helix. Also, although possibly a gross oversimplification, the C-terminus may or may not move from the closed position when the channel opens (Fig. 2 *B*).

Calculation of equivalent net charges of single domains of the MscL monomer

The MscL monomer consists of 136 amino acid residues deduced from its gene (Sukharev et al., 1994a). Hydropathy analysis revealed a highly hydrophobic protein with an amphipathic N-terminus (residues 1–15), followed by a highly hydrophobic segment (19–38), an amphipathic segment (50–69), a second highly hydrophobic segment (70–96), and a hydrophilic C-terminus (97–136) containing a cluster of charged residues RKKEE (104–108) (Sukharev et al., 1997). Secondary structure analysis (Arkin et al., 1997) together with the PhoA-fusion method analysis (Blount et al., 1996a) led to a working membrane spanning model of the MscL monomer comprising five structural domains denoted as S1, M1, S2-S3, M2, and C domain (Fig. 1 *A*) (Sukharev et al., 1996, 1997; Blount et al., 1996a). For the purposes of the EMC model we calculated the overall electric charge of each of the five domains by representing each of the S1, M1, M2, and S3 domain by a helical wheel (Fig. 1 *B*), and assuming no particular secondary structure for S2 and C domain. Also, we estimated the relative positions of these charges within each domain of the membrane-spanning MscL model (Fig. 2, *C* and *D*) by taking into account that an α-helix has an interturn distance of 5.4 Å corresponding to an advancement of ~1.5 Å per amino acid residue along the helix (Sybesma, 1977;

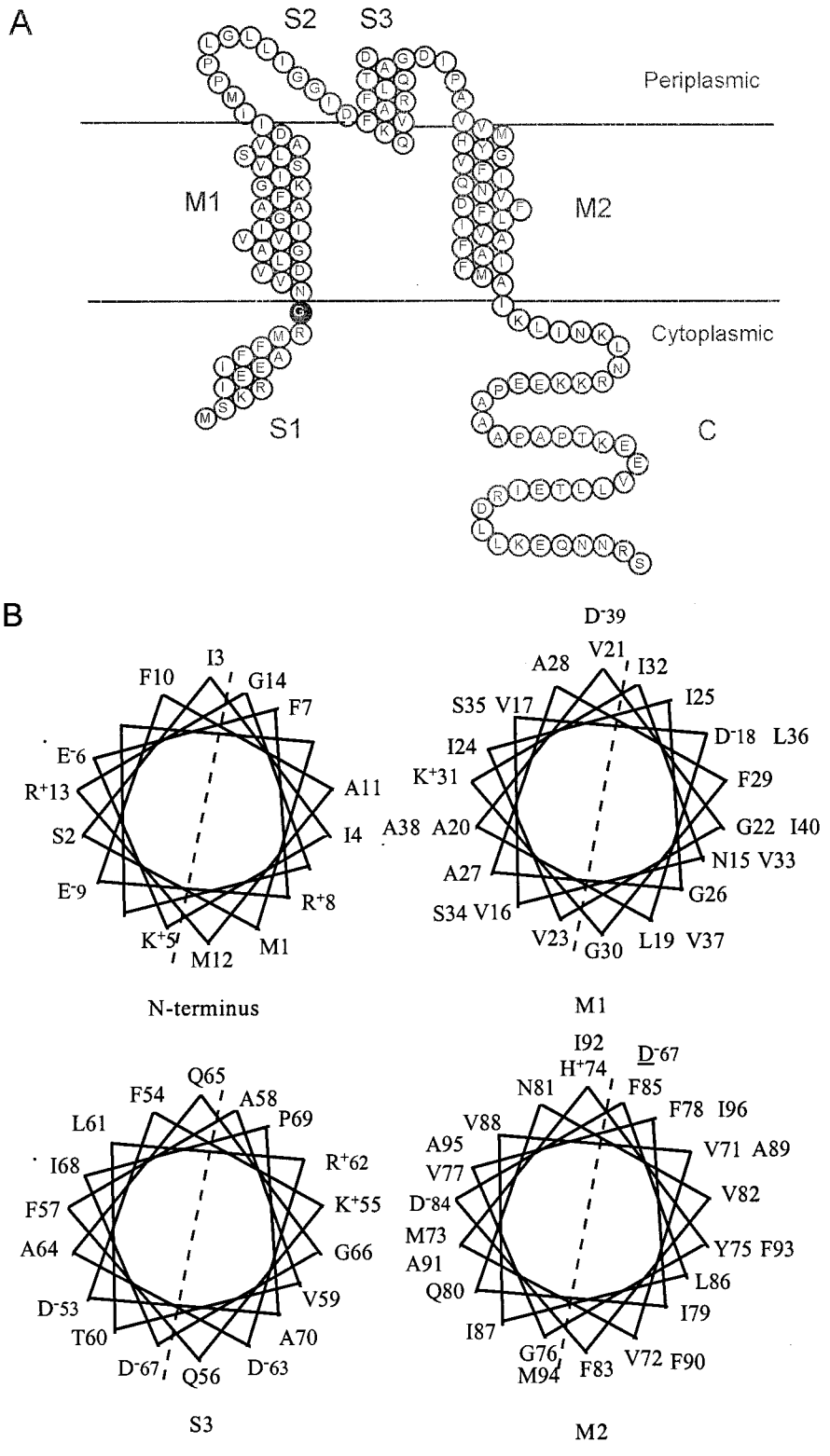

FIGURE 1 Structure of the MscL monomer. (*A*) A working topological model of the MscL monomer. The N-terminus (S1 domain) is proposed to form a cytoplasmic amphipathic α-helix; M1 and M2 domains represent the hydrophobic transmembrane α-helices. A glycine (Gly14, *black circle*), which is located near the N-terminus and M1 domain interface, is assumed to serve as a hinge in the proposed EMC gating model. (*B*) Amino acids of the N-terminus and M1 and M2 domains are arranged in an α-helical wheel of ~3.9 turns for the N-terminus and 7.4 turns for each of the M1 and M2 helices. Left sides in the N-terminus and M2 helix, and the right side in the M1 helix (*dashed line*) are more hydrophilic than the opposite side. Charged amino acids are marked by superscripts. The aspartate D67 (underlined) in M2 is the charged amino acid of the upper neighboring turn of the α-helix.

Geoffrey et al., 1988). The calculations of these model parameters are summarized in Table 1.

Using the helical wheel presentations in Fig. 1 *B* we estimated the net charges within the MscL monomer to be $+1e$ and $-1e$ for N-terminus and M1 domain, respectively. The M1 domain, S2-S3 loop, and M2 domain most likely follow the general helix-loop-helix model (Sukharev et al., 1997). Consequently, the aspartate D67 in the S3 domain may electrically neutralize the histidine H74 in the M2 domain, as they are in a close apposition to each other in the neighboring helices (Fig. 1 *B*). In that case the net charge of the M2 domain is $-1e$, and the net charge of the S2-S3 loop is zero. Otherwise, the net charge of M2 will be zero, and $-1e$ will be the net charge of the loop domain. Its equivalent position would then be determined by the aspartate D67, as the other oppositely charged amino acids are close to each other according to their α-helical structure. There-

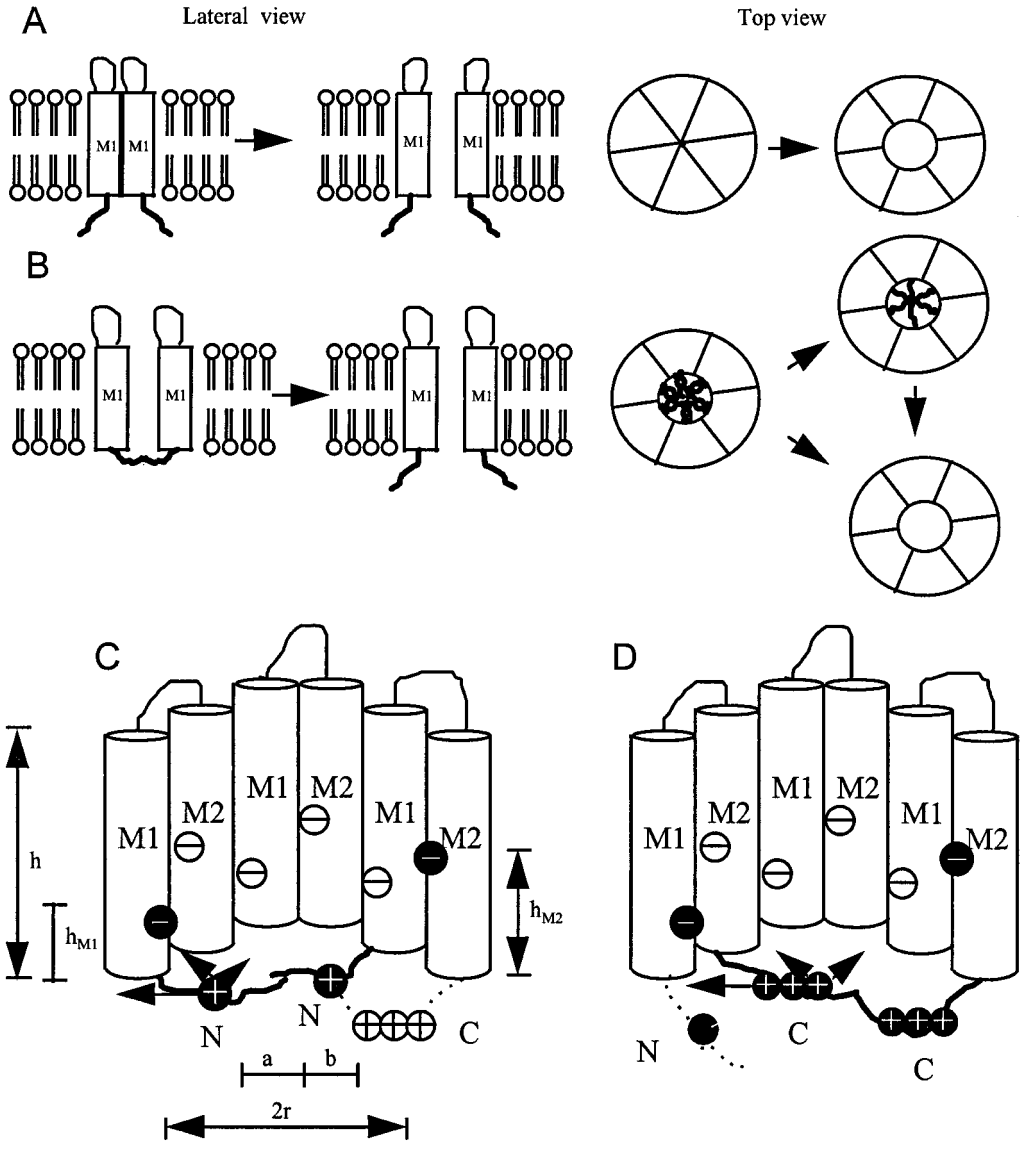

FIGURE 2 Model comparison. (*A*) A model in which the simultaneous "en bloc" displacement of all six monomers upon membrane stretch is responsible for the opening of the channel pore (Sukharev et al., 1997). (*B*) The ECM model proposes that a swing-like movement of the N-terminus is the major component responsible for the opening of the channel. (*C*) Net equivalent charges and their positions used for calculations in the ECM model: $2r = 40$ Å, $a = 11.25$ Å, $b = 2$ Å, $h = 40$ Å, $h_{M1} = 4.5$ Å, $h_{M2} = 18.75$ Å (see Table 1). Only three MscL subunits are shown for clarity. The electrostatic forces acting on the N-terminus are illustrated for one subunit of the MscL. To illustrate the electrostatic forces clearly, N- or C-termini are represented by dashed lines in the closed (*C*) and open (*D*) channel configuration.

fore, we calculated the electrostatic forces by considering both possibilities. In addition, it is not known how deep the S2-S3 loop may protrude into the channel pore inside the membrane bilayer. Thus, when the loop was considered for calculation, two possibilities were taken into account for the position of the loop S2 and the helix S3 relative to the membrane surface (see Table 3). Also, to simplify the calculation, the aspartate D67 was assumed to be equally distant from M1 and M2 domains, so that the horizontal component of the electrostatic force it exerts on the N- or C-terminus could be ignored. The C-terminus is highly hydrophilic and most likely located intracellularly (Fig. 1). Deletion of amino acid residues of Δ110–136 had no effect on channel function and gating (Blount et al., 1996b; Häse et al., 1997). However, the charged residues R104, K105, K106, E107, and E108 were found to be very important for channel function, because a deletion of residues from 104 on in the Δ104 C-terminal deletion mutant abolished the channel activity (Blount et al., 1996b; Häse et al., 1997). Therefore, we only considered the residues 96–110 to calculate the net equivalent electric charge of $+3e$ for the C-terminus (Table 1).

Electrostatic force analysis

Table 1 lists the parameters used in the model calculations. See also Fig. 3, *A* and *B*.

In the closed state, the main electrostatic forces acting on one N-terminus come from the other five N-termini, six C-termini, six M1 domains, and six M2 or S2-S3 (loop) domains in a closed channel. As shown in Results, in the case that the net charge of $-1e$ for M2 is considered, the effect of S2-S3 can be neglected, while in the case that the contribution of S2-S3 is taken into account, the net charge of M2 can be neglected.

TABLE 1 Parameters used in the EMC model calculations

Q_N	$+1e$	Equivalent net charges of N-termini
Q_C	$+3e$	Equivalent net charges of C-termini
Q_{M1}	$-1e$	Equivalent net charges of M1 transmembrane domain
Q_{M2}	$-1e$	Equivalent net charges of M2 transmembrane domain
Q_{loop}	$-1e$	Equivalent net charges of S2-S3 (loop) domain
r	~20 Å*	Radius of the MscL channel pore
a	~11.25 Å#	Distance between the N-terminal equivalent net positive charge and the N-terminus end (2.1 α-helical turn)
b	~2 Å#	Distance between the C-terminal equivalent net positive charge and the C-terminus end
h	~40 Å#	Height of the transmembrane domains (7.4 α-helical turn)
h_{M1}	~4.5 Å#	Distance from the equivalent net negative charge of the M1 domain to the joint of the M1 with the N-terminus (0.83 α-helical turn)
h_{M2}	~18.75 Å#	Distance from the equivalent net negative charge of the M2 domain to the joint of the M2 with the C-terminus (3.46 α-helical turn)
h_{loop}	40–60 Å	Depth of the S2-S3 domain inside the pore
D	4.5–5.2 μm§	Diameter of a membrane patch formed in a pipette tip
R		Radius of curvature of a membrane patch
γ		Membrane tension
p		Externally applied negative pressure (suction)
P_o		Channel open probability
A		Area of a membrane patch
s		Area of the MscL channel pore
K_L	0.14 N/m¶	Egg lecithin membrane elastic modulus

*Cruickshank et al., 1997.
#Positions of equivalent charges within single MscL domains were calculated using α-helix structural information according to Sybesma, 1977, and Geoffrey et al., 1988.
§Sokabe et al., 1991.
¶Kwok and Evans, 1981.

The sum of horizontal coulomb forces F_H is composed of each of the forces originating in other N-termini (F_{HN}), C-termini (F_{HC}), M1 (F_{HM1}), and M2 (F_{HM2}):

$$F_H = F_{HN} + F_{HC} + F_{HM1} + F_{HM2}$$

In the case that the net charge of M2 is zero, and S2-S3 net charge of $-1e$ is considered, the horizontal component of S2-S3 to the F_H can be ignored, so that it follows:

$$F_H = F_{HN} + F_{HC} + F_{HM1}$$

The sum of vertical components of coulomb forces F_V derives from the contribution of M1 (F_{VM1}), and M2 (F_{VM2}), or S2-S3 (F_{loop}):

$$F_V = F_{VM} = F_{VM1} + F_{VM2}$$

or

$$F_V = F_{VM} = F_{VM1} + F_{Loop}$$

All the electrostatic components are calculated in the following section.

Fig. 3 *A* shows the plane view of electrostatic interactions within the MscL homohexemeric pore. F_{HN}, the sum of the coulomb forces originating in five other N-termini and acting on each N-terminus, is given as:

$$F_{HN} = \sum_{i=2}^{6} f_{HN}^i$$

where

$$f_{HN}^i = \frac{Q_N^2}{4\pi\epsilon\epsilon_0 (l_N^i)^2} \cdot \cos(\phi_N^i)$$

where l_N^i denotes the distance between N_1 and N_2 and ϕ_N^i denotes the angle between the coulomb force and its horizontal component f_{HN}^i. All five horizontal components are described as follows:

$$f_{HN}^2 = f_{HN}^6 = \frac{Q_N^2}{4\pi\epsilon\epsilon_0 a^2}\left[\frac{\cos(\pi/3)}{2 - 2\cos(\pi/3)}\right]$$

$$f_{HN}^3 = f_{HN}^5 = \frac{Q_N^2}{4\pi\epsilon\epsilon_0 a^2}\left[\frac{\cos(\pi/6)}{2 - 2\cos(2\pi/3)}\right]$$

$$f_{HN}^4 = \frac{Q_N^2}{4\pi\epsilon\epsilon_0 a^2}\left[\frac{1}{2 - 2\cos(\pi)}\right]$$

The total contribution of six C-termini to the horizontally oriented forces acting on each N-terminus is:

$$F_{HC} = \sum_{i=1}^{6} f_{HC}^i$$

where

$$f_{HC}^i = \frac{Q_N Q_C}{4\pi\epsilon\epsilon_0 (l_C^i)^2} \cos(\phi_C^i)$$

Each component can be written as

$$f_{HC}^1 = f_{HC}^6 = \frac{Q_N Q_C}{4\pi\epsilon\epsilon_0}\left[\frac{a - b\cos(\pi/6)}{[a^2 + b^2 - 2ab\cos(\pi/6)]^{3/2}}\right]$$

$$f_{HC}^2 = f_{HC}^5 = \frac{Q_N Q_C}{4\pi\epsilon\epsilon_0}\left[\frac{a - b\cos(\pi/2)}{[a^2 + b^2 - 2ab\cos(\pi/2)]^{3/2}}\right]$$

$$f_{HC}^3 = f_{HC}^4 = \frac{Q_N Q_C}{4\pi\epsilon\epsilon_0}\left[\frac{a - b\cos(5\pi/6)}{[a^2 + b^2 - 2ab\cos(5\pi/6)]^{3/2}}\right]$$

Because N- and C-termini are both net positively charged, the total horizontal repulsive force between them drives the N-terminal domains out of the channel pore.

Fig. 3 *B* shows the electrostatic field analysis along the vertical axis of M1 and M2 domains. Each N-terminus (positively charged) is electrostatically attracted by the resultant force F_{M1M2} originating in six net negatively charged M1 and six M2 transmembrane domains. F_{M1M2} can be decomposed into horizontal (along the membrane surface) and vertical (membrane orientation) components:

$$\bar{F}_{M1M2} = \bar{F}_{HM} + \bar{F}_{VM}$$

F_{HM}, the total contribution of horizontal components originating from M1

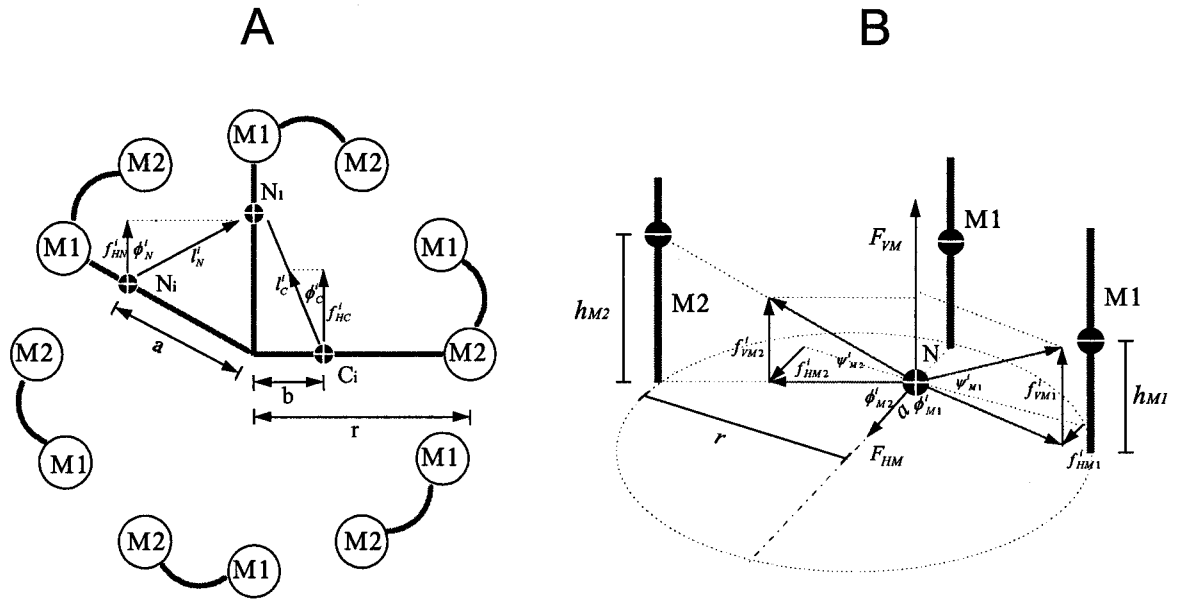

FIGURE 3 Electrostatic force analysis. (*A*) Top view of the coulomb forces and their corresponding horizontal components acting upon a single N-terminus of the MscL homohexamer in the plane of the membrane. (*B*) Cross-sectional view of the coulomb forces and their corresponding vertical components acting upon a single N-terminus.

and M2 transmembrane domains, and F_{VM}, the total contribution of vertical components originating from M1 and M2 domains, are given by

$$F_{HM} = \sum_{i=1}^{6} f^{i}_{HM1} + \sum_{i=1}^{6} f^{i}_{HM2}$$

where f^{i}_{HM1} and f^{i}_{HM2} are the individual horizontal components of electrostatic forces between N-termini and M1 and M2 domains.

$$f^{i}_{HM1} = \frac{Q_N Q_{M1}}{4\pi\epsilon\epsilon_0 (l^{i}_{M1})^2}\cos(\psi^{i}_{M1})\cos(\phi^{i}_{M1})$$

$$f^{1}_{HM1} = \frac{Q_N Q_{M1}}{4\pi\epsilon\epsilon_0}\left[\frac{a-r}{[(r-a)^2 + h^2_{M1}]^{3/2}}\right]$$

$$f^{2}_{HM1} = f^{6}_{HM1} = \frac{Q_N Q_{M1}}{4\pi\epsilon\epsilon_0}\left[\frac{a - r\cos(\pi/3)}{[r^2 + a^2 - 2ra\cos(\pi/3) + h^2_{M1}]^{3/2}}\right]$$

$$f^{3}_{HM1} = f^{5}_{HM1} = \frac{Q_N Q_{M1}}{4\pi\epsilon\epsilon_0}\left[\frac{a - r\cos(2\pi/3)}{[r^2 + a^2 - 2ra\cos(2\pi/3) + h^2_{M1}]^{3/2}}\right]$$

$$f^{4}_{HM1} = \frac{Q_N Q_{M1}}{4\pi\epsilon\epsilon_0}\left[\frac{a+r}{[(r+a)^2 + h^2_{M1}]^{3/2}}\right]$$

and

$$f^{i}_{HM2} = \frac{Q_N Q_{M2}}{4\pi\epsilon\epsilon_0 (l^{i}_{M2})^2}\cos(\psi^{i}_{M2})\cos(\phi^{i}_{M2})$$

$$f^{1}_{HM2} = f^{6}_{HM2} = \frac{Q_N Q_{M2}}{4\pi\epsilon\epsilon_0}\left[\frac{a - r\cos(\pi/6)}{[r^2 + a^2 - 2ra\cos(\pi/6) + h^2_{M2}]^{3/2}}\right]$$

$$f^{2}_{HM2} = f^{5}_{HM2} = \frac{Q_N Q_{M2}}{4\pi\epsilon\epsilon_0}\left[\frac{a - r\cos(\pi/2)}{[r^2 + a^2 - 2ra\cos(\pi/2) + h^2_{M2}]^{3/2}}\right]$$

$$f^{3}_{HM2} = f^{4}_{HM2} = \frac{Q_N Q_{M2}}{4\pi\epsilon\epsilon_0}\left[\frac{a - r\cos(5\pi/6)}{[r^2 + a^2 - 2ra\cos(5\pi/6) + h^2_{M2}]^{3/2}}\right]$$

and

$$F_{VM} = \sum_{i=1}^{6} f^{i}_{VM1} + \sum_{i=1}^{6} f^{i}_{VM2}$$

where f^{i}_{VM1} and f^{i}_{VM2} are the individual vertical components of electrostatic forces between N-termini and M1 and M2 domains.

$$f^{i}_{VM1} = \frac{Q_N Q_{M1}}{4\pi\epsilon\epsilon_0 (l^{i}_{M1})^2}\sin(\psi^{i}_{M1})$$

$$f^{1}_{VM1} = \frac{Q_N Q_{M1}}{4\pi\epsilon\epsilon_0}\left[\frac{h_{M1}}{[(r-a)^2 + h^2_{M1}]^{3/2}}\right]$$

$$f^{2}_{VM1} = f^{6}_{VM1} = \frac{Q_N Q_{M1}}{4\pi\epsilon\epsilon_0}\left[\frac{h_{M1}}{[r^2 + a^2 - 2ra\cos(\pi/3) + h^2_{M1}]^{3/2}}\right]$$

$$f^{3}_{VM1} = f^{5}_{VM1} = \frac{Q_N Q_{M1}}{4\pi\epsilon\epsilon_0}\left[\frac{h_{M1}}{[r^2 + a^2 - 2ra\cos(2\pi/3) + h^2_{M1}]^{3/2}}\right]$$

$$f^{4}_{VM1} = \frac{Q_N Q_{M1}}{4\pi\epsilon\epsilon_0}\left[\frac{h_{M1}}{[(r+a)^2 + h^2_{M1}]^{3/2}}\right]$$

and

$$f^{i}_{VM2} = \frac{Q_N Q_{M2}}{4\pi\epsilon\epsilon_0 (l^{i}_{M2})^2}\sin(\psi^{i}_{M2})$$

$$f^{1}_{VM2} = f^{6}_{VM2} = \frac{Q_N Q_{M2}}{4\pi\epsilon\epsilon_0}\left[\frac{h_{M2}}{[r^2 + a^2 - 2ra\cos(\pi/6) + h^2_{M2}]^{3/2}}\right]$$

$$f^{2}_{VM2} = f^{5}_{VM2} = \frac{Q_N Q_{M2}}{4\pi\epsilon\epsilon_0}\left[\frac{h_{M2}}{[r^2 + a^2 - 2ra\cos(\pi/2) + h^2_{M2}]^{3/2}}\right]$$

$$f^{3}_{VM2} = f^{4}_{VM2} = \frac{Q_N Q_{M2}}{4\pi\epsilon\epsilon_0}\left[\frac{h_{M2}}{[r^2 + a^2 - 2ra\cos(5\pi/6) + h^2_{M2}]^{3/2}}\right]$$

The attractive coulomb force between the loop S2-S3, F_{loop}, and the N-terminus is determined as follows:

$$F_{Loop} = \frac{Q_N Q_{Loop}}{4\pi\epsilon\epsilon_0 (h_{Loop})^2}$$

The maximal horizontal component of the attractive coulomb forces between the S2-S3 region and one N-terminus would be equal to 0.004 $e^2/4\pi\epsilon\epsilon_0$ if S2-S3 domains are positioned deep into the channel pore closest to the N-termini. In that extreme case the strength of the horizontal components of the coulomb forces (0.004 $e^2/4\pi\epsilon\epsilon_0$) is an order of magnitude smaller than the strength of the vertical components (0.165 $e^2/4\pi\epsilon\epsilon_0$ − 0.168 $e^2/4\pi\epsilon\epsilon_0$) (Table 2). Therefore, the contribution of the horizontal electrostatic components was ignored for further model considerations.

RESULTS

Coulomb forces governing the MscL mode of operation

The major events that may be occurring when the channel undergoes the closed-to-open transition can be briefly summarized as follows. In the model the channel pore of 40 Å is assumed to be formed by 12 α-helices of the channel homohexamer (Cruickshank et al., 1997) and has approximately the same diameter in both closed and open channel configuration. Glycine residue G14 is supposed to function as a hinge around which the N-terminus can rotate out of the pore within certain range of space angles. Although the C-terminus could be moving too, the N-terminus is more likely to undergo a swing-like movement than the C-terminus, due to the rotational flexibility of the glycine G14. Therefore, for the sake of simplicity we calculated the resulting coulomb forces as acting exclusively on the N-terminus. All parameter calculations in this study were based on this simplifying assumption. Acting as a gating arm, the N-terminus is supposed to be positioned parallel to the membrane when the channel is closed (Fig. 4). In this conformation, both N- and C-termini form six gating pairs to keep the channel closed. When pressure is applied and the membrane is stretched, the six N-termini of the homohexamer are forced out of the channel pore by swinging around their glycines G14. This simultaneous outward movement of six N-termini leads to the "unplugging" of the channel pore providing for ions to flow down their electrochemical gradients.

In the closed state, the electrostatic forces acting on one of the six N-termini come from the other five N-termini, six C-termini, and six of each M1 and M2 domains (see Methods). Since the N- and C-termini are both positively charged and are assumed not to be compressed by the repulsive electrostatic forces they exert on each other in the membrane plane, the resulting effect of the total repulsive force acting between them is to push the N-termini out of the membrane plane and consequently unplug the channel when the membrane is stretched (see next section). The horizontal repulsive force resulting from the other five N-termini is designated F_{HN}. The total repulsive force acting on one N-terminus that results from six C-termini is designated F_{HC}. Each N-terminus with one equivalent positive charge is electrostatically attracted by six of each negatively charged M1 and M2 helices. The corresponding resulting attractive force is designated F_{M1M2}. By constructing a parallelogram of coulomb forces, F_{M1M2} can be presented as a sum of a horizontal component, F_{HM}, along the membrane surface and a vertical component, F_{VM}, orthogonal to the membrane plane:

$$\bar{F}_{M1M2} = \bar{F}_{HM} + \bar{F}_{VM}$$

The horizontal resultant coulomb force acting on one N-

TABLE 2 Calculated horizontal and vertical electrostatic components (in $e^2/4\pi\epsilon\epsilon_0$)

	F_{HN}	F_{HC}	F_{HM}	F_H	F_{VM}	F_{loop} (40 Å)	F_{loop} (60 Å)	θ
a*	0.014	0.145	0.008	0.168	0.011	—	—	3.8°
b#	0.014	0.145	0.005	0.165	0.007	0.004	—	4.1°
c§	0.014	0.145	0.005	0.165	0.007	—	0.002	3.0°

*−1e of M2 is included in electrostatic analysis, S2-S3 loop is not considered.

#M2 is excluded, −1e of S2-S3 is considered and assumed to protrude inside the aqueous pore to a distance of 40 Å between the net charge of S2-S3 and the N-terminus.

§M2 is not considered, −1e of S2-S3 is assumed to protrude outside the aqueous pore to a distance of 20 Å between the net charge of S2-S3 and N-terminus. 60 Å results from the thickness of the membrane (40 Å) and the height of the S3 helix (20 Å equals 13.5 amino acid residues arranged in an α-helix).

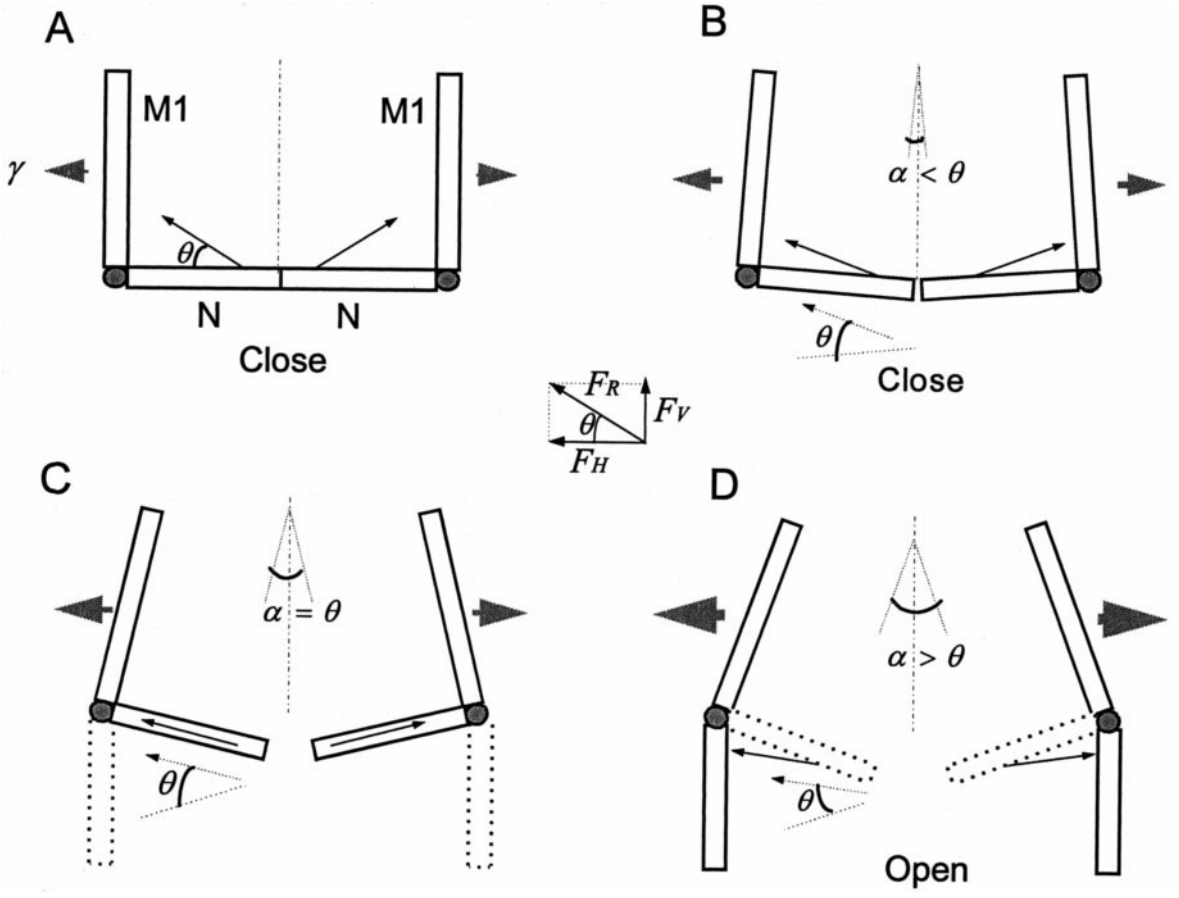

FIGURE 4 Electromechanical coupling mechanism. (*A*) No external pressure is applied. The resultant electrostatic force F_R is oriented in such a way that it encloses a very small angle $\theta \sim 3.8°$ with the gate plane formed by N-termini. The major effect of this force is to keep the gate closed; only two monomers of the MscL hexamer are shown for clarity. (*B*) External pressure is applied. The induced membrane tension γ pulls the monomers apart. The asymmetry of the charge distribution at the bottom and the top end of the channel hexamer causes them to tilt slightly at an angle α. As a consequence, the N-terminus will follow the M1 tilt at the same angle with a result that the angle between the N-terminus and the resultant coulomb force F_R becomes $\theta - \alpha$. (*C*) The increase in membrane tension pulls the single monomers apart at the angle $\alpha = \theta$. The orientation of the N-terminus and the resulting electrostatic force F_R are in the same direction. F_R pushes the N-terminus outward to rotate around G14 (*shaded circle*) out of the channel pore. The channel undergoes a transition from the closed to the open state. In this situation $P_o = 0.5$. (*D*) Larger membrane tension will cause tilting of the monomers at angles $\alpha > \theta$. F_R is more likely to induce the closed-open channel transition, such that open probability increases ($P_o > 0.5$).

terminus is therefore

$$F_H = F_{HN} + F_{HC} + F_{HM}$$

Another component, designated F_{loop}, that contributes to the electrostatic forces in a direction orthogonal to the membrane plane, originates from the net charge of six S2-S3 loops linking M1 and M2 domains. Thus, the sum of the orthogonal forces acting on one N-terminus is

$$F_V = F_{VM} + F_{Loop}$$

The values of all electrostatic components (F_{HN}, F_{HC}, F_{HM}, F_{VM}, and F_{loop}), and resulting horizontal (F_H) and vertical (F_V) forces (Table 2) were calculated using the parameters obtained from the working model of the MscL (Fig. 2, *C* and *D*). Details of the analysis are described in Methods.

Taking into account the results from Table 2 we can consider three different possibilities:

First, the equivalent net charge of M2 is $-1e$ and is positioned in the middle of M2, whereas the net charge of the S2-S3 loop is considered to be zero. In this case, the comparison of the relative strength of all electrostatic components indicates that of the three horizontal repulsive coulomb forces, the major repulsion comes from the electrostatic contribution of the N-termini (F_{HN}) and C-termini (F_{HC}). In comparison, both the horizontal (F_{HM}) and vertical (F_{VM}) attractive components coming from M1 and M2 are, in comparison, much weaker. The directions of F_H, F_V, and their resultant F_R are demonstrated in Fig. 4. The calculated angle θ between F_H and F_R is very small:

$$\theta = \arccos\frac{F_H}{F_R} = \arctan\frac{F_V}{F_H} = 3.8°$$

Second, the equivalent net charge of M2 is zero. The electrostatic attraction of M2 is therefore negligible. In-

stead, there is a net charge of $-1e$ in the S2-S3 domains. We may assume a case in which the loop region enters halfway into the channel pore formed by transmembrane helices. In this situation the negative charge of the aspartate D67 will be located near the entrance of the channel pore and the resulting vertical electrostatic force will increase because of the shorter distance between the equivalent net charges of N-termini and the S2-S3 loop. As shown in the second raw b in Table 2 the angle θ enclosed by F_H and F_R is in this case 4.1°, slightly larger than in the previous case (3.8°).

Third, the equivalent net charge of M2 is zero, the same as the former case, but the S2-S3 loops are assumed not to enter into the pore region. In this situation, in contrast to the previous case, the resulting vertical electrostatic force decreases due to the greater distance between the N-termini and the loops. The third raw c in Table 2 shows the calculation for this consideration. The angle θ enclosed by F_H and F_R is 3.0°, slightly smaller than in the previous cases.

A comparison of the relative strengths of all electrostatic components points toward an important result. In all cases considered, the angle θ between F_H and F_R varies within a very narrow range (~3.0°–4.1°). This result presents the basis for the EMC model of the MscL gating by mechanical force.

Tension-triggered electromechanical coupling mechanism

Fig. 2 *B* shows the diagram depicting the basic idea of the proposed EMC gating model. In the diagram the MscL channel pore with a diameter of 40 Å (Cruickshank et al., 1997) does not change significantly in size when the channel is closed or open. The swing-like movement of the N-terminus is assumed to dominate the gating process of the channel and should correspond to the open-close transition of the channel. In succession, the inclination of the single channel monomers caused by membrane tension (Fig. 4) acts as a "trigger" to initiate the N-terminal swing-like movement. The electrostatic coulomb forces existing between the single structural domains of the channel monomers carry sufficient energy to keep the channel closed, as well as to cause the swing-like movement of the N-termini. The net equivalent charges and their positions on the M1 and M2 domain, and N- and C-termini of the MscL homohexamer, are depicted in Fig. 2, *C* and *D*. Their corresponding values are given in Table 1.

Based on the distribution of coulomb forces in the closed state of the channel illustrated in Fig. 2, *C* and *D*, the MscL opening mechanism can be deduced as shown in Fig. 4. When no external pressure is applied to the patch pipette, the lipid membrane remains unstretched and forms an ideal planar lipid bilayer (Sokabe and Sachs, 1990; Sokabe et al., 1991). Twelve transmembrane helices (six M1 and six M2 α-helical domains) of the six MscL monomers form the 40-Å channel pore (Cruickshank et al., 1997). The pore is shut by the combined gate of N- and C-termini, both of which are assumed to lie horizontally within the pore parallel to the patch membrane. The resultant electrostatic force F_R is oriented in such a way that it encloses a very small angle θ with the gate plane formed by N- and C-termini. The resulting effect of this force is to keep the gate closed (Fig. 4 *A*).

When the negative pressure is applied to the pipette, the area of the membrane patch becomes enlarged. The increase in membrane tension provides a stimulus to pull the channel monomers away from each other, such that they become inclined toward the membrane plane in the tension direction. The angle at which they become tilted relative to each other is α (Fig. 4). Consequently, the N-terminus will also become tilted at the same angle with a result that the angle between a single N-terminus and the resulting coulomb force F_R becomes $\theta - \alpha$ (Fig. 4 *B*). The hypothesis that membrane tension should cause the monomers to tilt in the particular direction is based on our calculations of electrostatic interactions between the channel domains. The calculations indicate that the repulsive coulomb forces at the N- and C-terminal end of the channel are larger than at the opposite end. When the membrane is stretched and the monomers are pulled apart, the asymmetry of the charge distribution at the two ends of the channel hexamer would be expected to cause a predominant spreading of the monomers at the bottom end such that they become tilted, as suggested in our model.

When the applied external pressure exceeds a certain level such that the pull on the single monomers caused by membrane tension tilts the M1 and M2 helices to a degree that α becomes equal to θ (Fig. 4 *C*), the orientation of F_R to the N-terminus will start to change in a direction to pull the N-terminus downward out of the channel pore (Fig. 4 *D*). In this case, the channel undergoes a transition from the closed to the open state. In reality, because of the intrinsic thermal energy kT, the θ and α defined in this model are the average values of corresponding angles over time. Therefore, even at lower applied pressures at which α is less than θ (Fig. 4 *B*), the channel still has a finite probability to reach open state at certain time t, when its instantaneous value α_t becomes greater than θ_t. This probability could be considered to correspond to the channel open probability (P_o) obtained at the particular negative pressure applied to the patch clamp pipette. Consequently, at pressures at which α is equal to θ, open probability should be $P_o = 0.5$.

In summary, the mechanosensation of MscL results from coupling of mechanical and electrostatic forces, such that relative movements of the channel domains affects electrostatic interactions between these domains. The applied pressure provides a mechanical external stimulus that causes an increased membrane tension. Due to lipid-protein interactions, membrane tension causes an inclination of the channel monomers toward each other. This slight tilting of the transmembrane domains may serve as a trigger to initiate the outward movement of the N-terminal domain caused by

electrostatic repulsion between N- and C-termini. This results in the channel opening.

Activation pressure

To test the feasibility of the ECM model we calculated the pressure p needed to produce a tilt of the channel monomers at an angle α relative to each other (Fig. 4). For an ideal membrane patch, the relationship between external pressure p and the membrane tension γ is

$$p = \frac{2\gamma}{R}, \tag{1}$$

where R is the radius of curvature of a membrane patch under pressure p. The membrane tension γ is determined by the elasticity constant K_L, and the fractional increase of membrane area $\Delta A/A$

$$\gamma = \frac{K_L \Delta A}{A}. \tag{2}$$

The area of a relaxed lipid membrane patch having a diameter D equal to the pipette diameter is

$$A = \pi D^2/4. \tag{3}$$

When external negative pressure (suction) is applied to the patch pipette, the surface of the stretched membrane increases by a fraction corresponding to the area of a sphere with a radius of curvature R. The area of the spherical calotte is:

$$A' = 2\pi R(R - \sqrt{R^2 - D^2/4}). \tag{4}$$

The fractional increase of membrane area $(\Delta A/A) = (A' - A/A)$ due to the stretch of the membrane can be calculated and the relationship between applied pressure p and the radius of curvature can be obtained using Eqs. 1–4.

$$p = \frac{2K_L[2R(R - \sqrt{R^2 - D^2/4}) - D^2/4]}{RD^2/4}. \tag{5}$$

The increase of membrane patch area generates membrane tension γ, which causes the transmembrane domains of MscL to tilt at an inclination angle α along the tension direction, which results in an increase of the area of the channel pore $\Delta s = s' - s$, where $s = r^2\ \pi \approx 1200$ Å^2 (Cruickshank et al., 1997). The fractional increase in pore area is assumed to be equal to the fractional increase of the membrane patch:

$$\frac{\Delta A}{A} = \frac{\Delta s}{s} = \frac{s' - s}{s}. \tag{6}$$

The limitation of this assumption is that the elastic properties of the channel protein and the surrounding membrane bilayer are assumed to be similar. Despite that limitation, we used this assumption to provide a bridge between structural changes within the channel molecule and macroscopic area changes in the membrane patch. The channel pore radius in the closed state is $r = 20$ Å. The area is

$$s = \pi r^2 \tag{7}$$

Taking into account that the tilt of the monomers relative to each other under membrane tension (Fig. 4) would cause a slightly conical shape of the channel pore, the average enlarged area of the pore, s', can be described as

$$s' = \pi(r + \Delta r/2)^2 \tag{8}$$

where Δr is the increase of the pore radius, and is determined by

$$\Delta r = h \cdot \tan(\alpha/2) \tag{9}$$

It follows:

$$\frac{\Delta A}{A} = \frac{\Delta s}{s} = \frac{r \cdot \Delta r + \Delta^2 r/4}{r^2} \tag{10}$$

As described above, when $\alpha = \theta$, activation pressure is assumed to cause the channel to be open 50% of the time ($P_o = 0.5$). Thus we can correlate the radius of curvature R and pressure p with differences in the patch diameter D (Table 3).

The range of the calculated activation pressures is in good agreement with the negative pressure of ~65 mmHg required to activate the MscL 50% of the time in our experiments (Häse et al., 1995). However, we are uncertain about the radius of liposome patches formed inside our pipettes. The results in Table 3 indicate that the diameters of lipid membrane patches in pipettes formed in our experiments may range between 2 and 3 μm, which is in good agreement with the values reported in the literature (Sokabe et al.,

TABLE 3 Predicted activation pressure $p_{0.5}$ required for 50% channel activation in dependence of the radius of a membrane patch

		M2		S2-S3 (40 Å)		S2-S3 (60 Å)	
P (%)	D (μm)	R/0.5 D*	$p_{0.5}$ (mmHg)	R/0.5 D	$p_{0.5}$ (mmHg)	R/0.5 D	$p_{0.5}$ (mmHg)
0.5	2	2.0	69	1.9	76	2.3	49
0.5	3	2.0	48	1.9	51	2.3	33
0.5	4	2.0	35	1.9	38	2.3	25
0.5	5	2.0	28	1.9	31	2.3	20

*0.5 D represents the initial radius of the membrane patch.

1991). Also, the calculated values correspond well with our estimate of the size of the opening of the tip of pipettes of ~1 μm from the bubble number and pipette resistance (Cruickshank et al., 1997).

Energy calculation

The free energy ΔG is a linear function of membrane tension γ according to the model proposed by Howard et al. (1988),

$$\Delta G = \Delta G^0 + \gamma \cdot \Delta s \tag{11}$$

where ΔG^0 is the difference in free energy between the closed and open conformations of the channel in the absence of membrane tension, and Δs is the difference in membrane area occupied by these two conformations at a given membrane tension. When the open probability P_o = 0.5, free energy change = 0. Using Eqs. 2, 6, and 15, it follows:

$$\begin{aligned}\Delta\Delta G &= -\Delta G^0 \\ &= \gamma \cdot \Delta s = K_L \frac{\Delta^2 s}{s} \\ &= 8.3 \times 10^{-21}\, J \approx 2\, kT\end{aligned} \tag{12}$$

Thus, according to the EMC model the energy requirement to gate the MscL is minimal, since as little as 2 kT is sufficient to keep the channel open half of the time. This is consistent with a notion of very small molecular displacements of single channel domains underlying major conformational changes of the channel as a whole.

MscL mutants

We used the results obtained with several MscL mutants as a test for the consistency between the predictions of the ECM model and the experimentally observed results. An N-terminal deletion mutant NBE (Δ1-8) and an N-terminal substitution mutant P6 (first eight N-terminal residues substituted by nine novel amino acids, resulting in a less charged N-terminus compared to that of the wild-type MscL) were examined for their pressure sensitivity and gating properties (Häse et al., 1997). Both mutants exhibited a marked alteration in channel activation by pressure. A site-directed mutation, Q56R, which made the S2-S3 loop more positively charged, resulted in a channel that became more sensitive to the applied pressure (Blount et al., 1996a). Although the experiments by Blount and coworkers (1996a,b) were performed in giant spheroplasts usually requiring higher pressures to activate the MscL, a comparison of experimentally obtained values for pressure sensitivity of the corresponding mutants with the theoretical predictions calculated according to the EMC model shows, for the most part, a good agreement between the two sets of data (Table 4). One exception is the site-directed mutant K31D in the M1 helix (Blount et al., 1996b). In its present form the model cannot account for the increase in the MscL pressure sensitivity observed in this mutant.

DISCUSSION

How are MS ion channels gated by mechanical force? At present, two mechanisms of mechanosensitivity have been recognized (Hamill and McBride, 1997): the first, possibly more general mechanism, can be described according to the bilayer model (Martinac et al., 1990; Markin and Martinac,

TABLE 4 Predicted and measured half-activation pressure $p_{0.5}$ for membrane patches of the wild-type and various mutants of MscL

	M2		S2-S3 (40 Å)		S2-S3 (60 Å)		Measured Activation
	θ*	$p_{0.5}$ (mmHg)[#]	θ	$p_{0.5}$ (mmHg)	θ	$p_{0.5}$ (mmHg)	pressure $p_{0.5}$ (mmHg)
Wild Type[§]	3.8°	69	4.1°	76	3.0°	49	61.7 ± 28.6 (n = 3)
P6	9.7°	234	8.8°	218	7.0°	165	~157.7 ± 37.0[¶] (n = 7)
Δ104	10.6°	301	12.7°	387	9.6°	209	— (n = 16)
K31E	6.8°	158	6.2°	140	4.5°	117	43.4 ± 27.2[‖] ($n \geq 6$)
Q56R	2.4°	36	2.4°	36	2.4°	36	43.8 ± 27.5[‖] ($n \geq 6$)
Q56H (pH 7.5)	3.8°	69	4.1°	76	3.0°	49	52.9 ± 33.1[‖] ($n \geq 6$)
Q56H (pH 5.0)	2.4°	36	2.4°	36	2.4°	36	43.1 ± 27.0[‖] ($n \geq 6$)

[§]The initial diameter of a membrane patch is assumed to be 2 μm.

*θ is the angle enclosed by the resultant electrostatic force F_R and its horizontal component F_H (Fig. 3).

[#]$p_{0.5}$ (mmHg) is the activation pressure required for the 50% open probability.

[¶]The half-activation pressure was calculated using the value of 132.2 mmHg for the negative activation pressure at which the first full opening event of the mutant channel was observed (Häse et al., 1997) and the value of 4.5 ± 2.0 mmHg for the pressure sensitivity of the wild-type MscL (Häse et al., 1995; Cruickshank et al., 1997).

[‖]The half-activation pressure was calculated using the value of 36.2 ± 22.7 mmHg (n = 9) for MscS in giant *E. coli* spheroplasts (B. Martinac, unpublished data) and the values for the ratio of the pressure activation between MscL and MscS (K31E: 1.20 ± 0.04; Q56R: 1.21 ± 0.04; Q56H (pH 7.5): 1.46 ± 0.03; Q56H (pH 5.0): 1.19 ± 0.03) (Blount et al., 1996b).

1991; Opsahl and Webb, 1994), whereas the second, possibly more specialized mechanism, is best represented by the tethered model (Guharay and Sachs, 1984; Howard et al., 1988; Hudspeth and Gillespie, 1994; Hamill and McBride, 1996). The bilayer and the tethered model both were proposed at the time when no knowledge was available on structure and function relationships for any MS ion channel. Consequently, both models suffice only to account for the mechanosensitivity of MS channels at a phenomenological descriptive level, but cannot account for the underlying molecular mechanism(s).

In the case of MscL the gating mechanism complies with the bilayer model, since it was unambiguously demonstrated that MscL is gated by mechanical force that is exclusively transmitted via lipid bilayer alone (Sukharev et al., 1993; Häse et al., 1995). In addition, the primary structure of MscL is known (Sukharev et al., 1994a), and a topological multimeric membrane spanning model of MscL supported by ample experimental evidence has been proposed (Blount et al., 1996; Sukharev et al., 1994a, 1997). Also, a very recent patch clamp study using the recombinant MscL indicated further that the functional MscL channel is most likely a homohexamer with a pore size of ~40 Å (Cruickshank et al., 1997). Consequently, it should be possible to identify the molecular structures and mechanisms underlying the MscL mechanosensitivity. The electromechanical coupling (EMC) model thus presents the first attempt in this direction.

By using the EMC model we were able to calculate pressure sensitivities and open probabilities expected for the wild-type and several mutants of the MscL. The obtained theoretical results were in close agreement with most of the currently available experimental data (see Tables 2–4). Therefore, in its essence the MscL mechanosensitivity and its mode of operation may be explained by two consecutive molecular events leading to the channel opening. First, the pressure-induced membrane tension causes the single monomers of the channel homohexamer to become tilted relative to each other. We calculated the corresponding inclination angle to be ~3.0°–4.1°. For comparison, a clockwise rotation at an angle of 3.8° and 3.9° of the two α-subunits of the nicotinic AchR channel was shown to cause this channel to open (Unwin, 1995) indicating that minute molecular displacements of the structural channel elements should suffice for major conformational changes of the channel macromolecule, such as "open ↔ closed" transition. Second, the relative displacement of the monomers and corresponding transmembrane M1 and M2 domains causes the N-termini of the channel multimer to turn away from each other and from other domains in a swing-like movement, causing the channel to open. It is also possible that C-termini might be moving too far away from the channel pore, thus, together with the N-termini, unplugging the pore (Fig. 2 *B*). However, without knowing the tertiary structure of the channel, the simplest assumption that was consistent with the present experimental evidence is that only N-termini move induced by the electrostatic repulsion by the overall positively charged six C- and the remaining five N-termini. This conclusion seems to be consistent with the calculation of the minimal energy of 2 kT being sufficient to open the channel.

The question that remained unanswered by the EMC model in its present form is how the channel should close after the removal of membrane tension. With no experimental evidence on specific interactions between the channel molecule and the surrounding lipids, we are not in a position to properly answer the question about the particular molecular mechanism(s) governing the channel closing. However, from the experiment we know that the channel remains closed without applied pressure, since the pressure (membrane tension) is required to open the channel. Obviously, the physics of the system indicates that in the closed configuration the channel possesses minimum free energy stabilizing this protein conformation in respect to its lipid surroundings. If among all possible types of protein-lipid interactions we only assume multiple nonspecific, low-energy interactions between the acyl chains of the "boundary lipids" and the hydrophobic amino acids of MscL, we could expect at least 10–20 kT of energy of interaction stabilizing the channel structure. This is because the nonspecific interactions are best described by van der Waals forces and steric interactions (Selinsky, 1992). Taking into account that interaction energies due to van der Waals forces are ~4–8 KJ/mol, this would correspond to $\sim 40-80 \times 10^{-21}$ J/hexamer = 10–20 kT. This amount of energy could provide for stabilization of the secondary and tertiary channel structure and should suffice to overcome the ≤ 2 kT of the net repulsive electrostatic forces that open the channel. Consequently, the channel should be able to close when membrane tension is removed. The following argument may further clarify that 2 kT should be sufficient to operate the closed ↔ open transition of the channel.

The calculation of membrane tension γ using Eq. 1 is correct only if 1) the tension γ is calculated for an ideal biological membrane that is well approached by liposome patches in reconstitution experiments, and 2) the radius of membrane curvature is not constant, but a function of the applied pressure. For example, when several mmHg pressure is applied to a membrane patch with a diameter D, what will the membrane tension be? To calculate the membrane tension we cannot use the diameter D of the membrane patch in the absence of the applied pressure. To calculate the membrane tension γ produced in the patch by a constant pressure p, we used Eqs. 2–5. In a medium-sized pipette having a typical diameter of 0.8–1.0 μm and resistance of 4–6 MΩ, patches are usually located 8–15 μm from the tip and have diameters in a range between 4.2 and 5.2 μm when no negative pressure (suction) is applied (Sokabe and Sachs, 1990; Sokabe et al., 1991). Based on these considerations a pressure of 5 mmHg applied to a "flat" patch with a diameter of 4.2–5.2 μm will stretch the patch to become curved with a radius of curvature of 8.1–9.2 μm. Taking into

account that pressure of 5 mmHg is sufficient to produce an *e*-fold change in open probability of the MscL (Häse et al., 1995) the expected average increase in the area of the pore Δs will be $\sim 25\pi$ Å^2 ($=78.5$ Å^2). From this change in the area of the channel pore the expected change in the radius of the pore should be $\Delta r = 1.85$ Å (Eqs. 7 and 8). Such a small change in the pore radius is inconsistent with the model shown in Fig. 2 *A*, in which the MscL homohexamer undergoes a conformational change corresponding to a displacement of all 12 helices of the homohexamer from the channel, having a radius $r = 0$ in a closed state to an open channel with a pore of 40 Å in diameter (Cruickshank et al., 1997). In contrast, according to the ECM model the range of negative pressures in our experiments could suffice to induce the unplugging of the already existing 40 Å cylindrical pore via a swing-like movement of the N-terminus away from the pore. Therefore, the N-terminus may literally play a *pivotal* role in the MscL gating. Finally and most importantly, although it cannot account for all available experimental evidence, such as in the case of the K31D mutant, the EMC model provides a basis for a future design of novel MscL mutants to be used in structure and function experiments for a further test of the model itself.

Dr. L. Gu and Dr. W. Liu contributed equally to this work. Also, we thank our colleagues Dr. N. Saint and Dr. A. C. Le Dain and other members of the laboratory including A. Kloda, C. C. Cruickshank, and S. J. Butterly, as well as Dr. J. W. Deitmer (University of Kaiserslautern) for helpful discussion and critical reading of the manuscript.

This work was supported by grants from the Australian Research Council (A19332733) and the National Health and Medical Research Council of Australia (960591).

REFERENCES

Arkin, I. T., S. I. Sukharev, P. Blount, C. Kung, and A. T. Brünger. 1997. Helicity, membrane incorporation, orientation, and thermal stability of the large mechanosensitive ion channel from *E. coli*. *J. Biol. Chem.* (in press).

Berrier, C., M. Besnard, B. Ajouz, A. Coulombe, and A. Ghazi. 1996. Multiple mechanosensitive ion channels from *Escherichia coli*, activated at different thresholds of applied pressure. *J. Membr. Biol.* 151:175–187.

Blount, P., S. I. Sukharev, P. C. Moe, S. K. Nagle, and C. Kung. 1996c. Towards an understanding of the structural and functional properties of MscL, a mechanosensitive channel in bacteria. *Biol. Cell.* 87:1–8.

Blount, P., S. I. Sukharev, P. C. Moe, M. J. Schroedeer, H. R. Guy, and C. Kung. 1996a. Membrane topology and multimeric structure of a mechanosensitive channel protein of *Escherichia coli*. *EMBO J.* 15:101–108.

Blount, P., S. I. Sukharev, M. J. Schroedeer, S. K. Nagle, and C. Kung. 1996b. Single residue substitutions that change gating properties of a mechanosensitive channel in *Escherichia coli*. *Proc. Natl. Acad. Sci. USA.* 93:11652–11657.

Branden, J., and J. Tooze. 1991. Introduction to Protein Structure. Garland Publishing Inc., New York and London.

Cruickshank, C. C., R. F. Minchin, A. C. Le Dain, and B. Martinac. 1997. Estimation of the pore size of the large-conductance mechanosensitive ion channel (MscL) of *Escherichia coli*. *Biophys. J.* 73:1925–1931.

García-Añoveros, J., and D. P. Corey. 1997. The molecules of mechanosensation. *Annu. Rev. Neurosci.* 20:567–594.

Geoffrey, Z., F. R. Salemme, and I. Geis. 1988. The three-dimensional structures of proteins. *In* Biochemistry, 2nd ed. Macmillan Publishing Company, New York. 53–59.

Guharay, F., and F. Sachs. 1984. Stretch-activated single ion channel currents in tissue-cultured embryonic chick skeletal muscle. *J. Physiol. (Lond).* 352:685–701.

Hamill, O. P., A. Marty, E. Neher, B. Sackmann, and F. J. Sigworth. 1981. Improved patch-clamp techniques for high-resolution current recording from cells and cell-free membrane patches. *Pflügers Arch. Eur. J. Physiol.* 391:85–100.

Hamill, O. P., and D. W. McBride, Jr. 1994. The cloning of a mechanogated membrane ion channel. *TINS.* 17:439–443.

Hamill, O. P., and D. W. McBride, Jr. 1996. The pharmacology of mechanogated membrane ion channels. *Pharmacol. Rev.* 48:231–252.

Hamill, O. P., and D. W. McBride, Jr. 1997. Induced membrane hypo/hypermechanosensitivity: a limitation of patch-clamp recording. *Annu. Rev. Physiol.* 59:621–631.

Häse, C. C., A. C. Le Dain, and B. Martinac. 1995. Purification and functional reconstitution of the recombinant large mechanosensitive ion channel (MscL) of *Escherichia coli*. *J. Biol. Chem.* 270:18329–18334.

Häse, C. C., A. C. Le Dain, and B. Martinac. 1997. Molecular dissection of the large mechanosensitive ion channel (MscL) of *E. coli*: mutants with altered channel gating and pressure sensitivity. *J. Membr. Biol.* 157: 17–25.

Howard, J., W. M. Roberts, and A. J. Hudspeth. 1988. Mechanoelectrical transduction by hair cells. *Annu. Rev. Biophys. Chem.* 17:99–124.

Hudspeth, A. J., and P. G. Gillespie. 1994. Pulling strings to fine tune transduction: adaptation by hair cells. *Neuron.* 12:1–9.

Kwok, R., and E. Evans. 1981. Thermoelasticity of large lecithin bilayer vesicles. *Biophys. J.* 35:637–652.

Markin, V. S., and B. Martinac. 1991. Mechanosensitive ion channels as reporters of bilayer expansion: a theoretical model. *Biophys. J.* 60: 1120–1127.

Martinac, B. 1993. Mechanosensitive ion channels: biophysics and physiology. *In* Thermodynamics of Membrane Receptors and Channels. M. B. Jackson, editor. CRC Press, Boca Raton, FL. 327–351.

Martinac, B., J. Adler, and C. Kung. 1990. Mechanosensitive ion channels of *E. coli* activated by amphipaths. *Nature.* 348:261–263.

Martinac, B., M. Buechner, A. H. Delcour, J. Adler, and C. Kung. 1987. Pressure-sensitive ion channel in *Escherichia coli*. *Proc. Natl. Acad. Sci. USA.* 84:2297–2301.

Martinac, B., A. H. Delcour, M. Buechner, J. Adler, and C. Kung. 1992. Mechanosensitive ion channels in bacteria. *In* Comparative Aspects of Mechanoreceptor Systems. F. Ito, editor. Springer Verlag. 3–18.

Morris, C. E. 1990. Mechanosensitive ion channels. *J. Membr. Biol.* 113: 93–107.

North, R. A. 1996. Families of ion channels with two hydrophobic segments. *Curr. Opin. Cell Biol.* 8:474–483.

Opsahl, L. R., and W. W. Webb. 1994. Transduction of membrane tension by the ion channel alamethicin. *Biophys. J.* 66:71–74.

Sachs, F. 1988. Mechanical transduction in biological systems. *CRC Crit. Rev. Biomed. Eng.* 16:141–169.

Sachs, F. 1992. Stretch-sensitive ion channels: an update. *In* Sensory Transduction. D. P. Corey and S. D. Roper, editors. Rockefeller University Press, New York. 242–260.

Sackin, H. 1995. Mechanosensitive channels. *Annu. Rev. Physiol.* 57: 333–353.

Selinsky, B. S. 1992. The Structure of Biological Membranes. P. Yeagle, editor. CRC Press, Boca Raton, FL. 603–651.

Sokabe, M., and F. Sachs. 1990. The structure and dynamics of patch-clamped membranes: a study using differential interference contrast light microscopy. *J. Cell Biol.* 111:599–606.

Sokabe, M., F. Sachs, and Z. Q. Jing. 1991. Quantitative video microscopy of patch clamped membrane stress, strain, capacitance, and stretch channel activation. *Biophys. J.* 59:722–728.

Sukharev, S. I., P. Blount, B. Martinac, F. R. Blattner, and C. Kung. 1994a. A large-conductance mechanosensitive channel in *E. coli* encoded by *mscL* alone. *Nature.* 368:265–268.

Sukharev, S. I., P. Blount, B. Martinac, H. B. Guy, and C. Kung. 1996. MscL: a mechanosensitive channel in *Escherichia coli*. *In* Organellar Ion

Channels and Transports, Vol. 51. D. E. Clapham and B. Ehrlich, editors. Society of General Physiologists, New York.

Sukharev, S. I., P. Blount, B. Martinac, and C. Kung. 1997. Mechanosensitive channels of *Escherichia coli*: the MscL gene, protein, and activities. *Ann. Rev. Physiol.* 59:633–657.

Sukharev, S. I., B. Martinac, V. Y. Arshavsky, and C. Kung. 1993. Two types of mechanosensitive channels in the *Escherichia coli* cell envelope: solubilization and functional reconstitution. *Biophys. J.* 65:177–183.

Sukharev, S. I., B. Martinac, P. Blount, and C. Kung. 1994b. Functional reconstitution as an assay for biochemical isolation of channel proteins: application to the molecular identification of a bacterial mechanosensitive channel. *Methods: A Companion to Methods Enzymol.* 6:51–59.

Sybesma, C. 1977. An Introduction to Biophysics. Academic Press, New York. 54.

Unwin, N. 1995. Acetylcholine receptor channel imaged in the open state. *Nature* 373:37–43.